Received: 1 April 2024 | Revised: 12 August 2024 | Accepted: 19 August 2024

DOI: 10.1002/nbm.5255

RESEARCH ARTICLE

NMR IN BIOMEDICINE WILEY

Repeatability of alkaline inorganic phosphate quantification in the skeletal muscle using ^{31}P-magnetic resonance spectroscopy at 3 T

Alexs A. Matias[1] | Corinna F. Serviente[1,2] | Stephen T. Decker[1,3] | Muhammet Enes Erol[1,4] | Gaia Giuriato[1,4,5,6] | Yann Le Fur[7] | Rajakumar Nagarajan[8,9] | David Bendahan[7] | Gwenael Layec[1,8,9]

[1]Department of Kinesiology, University of Massachusetts at Amherst, Amherst, MA, USA

[2]Diabetes & Metabolism Research Center, University of Utah, Salt Lake City, UT, USA

[3]The Institute for Applied Life Sciences, University of Massachusetts at Amherst, Amherst, MA, USA

[4]School of Health and Kinesiology, University of Nebraska at Omaha, Omaha, NE, USA

[5]Department of Neuroscience, Biomedicine, and Movement Science, University of Verona, Verona, Italy

[6]Department of Surgical, Medical and Dental, University of Modena and Reggio Emilia, Modena, Italy

[7]Department of Morphological Sciences Related to Transplant, Oncology and Regenerative Medicine, University of Modena and Reggio Emilia, Modena, Italy

[8]Centre de Resonance Magnetique Biologique et Medicale, UMR CNRS 6612, Faculté de Médecine de Marseille, Marseille, France

[9]Human Magnetic Resonance Center, Institute for Applied Life Sciences, University of Massachusetts at Amherst, Amherst, MA, USA

Correspondence
Gwenael Layec, PhD, Assistant Professor, School of Health and Kinesiology, University of Nebraska at Omaha, Omaha, NE, 6001 Dodge Street, H&K 207R, Omaha, NE 68182-0216, USA.
Email: glayec@unomaha.edu

Funding information
This work was funded in part by the NIH National Heart, Lung, and Blood Institute [R00 HL125756-03] (GL).

Abstract

The detection of a secondary inorganic phosphate (Pi) resonance, a possible marker of mitochondrial content in vivo, using phosphorus magnetic resonance spectroscopy (^{31}P-MRS), poses technical challenges at 3 Tesla (T). Overcoming these challenges is imperative for the integration of this biomarker into clinical research. To evaluate the repeatability and reliability of measuring resting skeletal muscle alkaline Pi (Pi_{alk}) using with ^{31}P-MRS at 3 T. After an initial set of experiments on five subjects to optimize the sequence, resting ^{31}P-MRS of the quadriceps muscles were acquired on two visits (~4 days apart) using an intra-subjects design, from 13 sedentary to moderately active young male and female adults (22 ± 3 years old) within a whole-body 3 T MR system. Measurement variability attributed to changes in coil position, shimming procedure, and spectral analysis were quantified. ^{31}P-MRS data were acquired with a ^{31}P/-proton (^{1}H) dual-tuned surface coil positioned on the quadriceps using a pulse-acquire sequence. Test–retest absolute and relative repeatability was analyzed using

Abbreviations: **Pi**, inorganic phosphate; **MR**, magnetic resonance; **T**, tesla; Pi_{alk}, alkaline inorganic phosphate; **CV**, coefficient of variation; **ICC**, Intra-class correlation coefficients; **ATP**, Adenosine Triphosphate; **PCr**, phosphocreatine; **PDE**, phosphodiesters; **PME**, phosphomonoester; **GPE**, glycerophosphoethanolamine; **GPC**, glycerophosphocholine; **NAD**, nicotinamide dinucleotide; Pi_{cyt}, cytosolic inorganic phosphate; **TA**, tibialis anterior; Q_{max}, ATP synthesis; **ppm**, parts per million; **mM**, millimolar; **ms**, milliseconds; **kHz**, kilohertz; **WALTZ-4**, wideband alternating-phase low-power technique for zero-residual splitting; **SAR**, specific absorption rate; **TR**, repetition time; **T1**, longitudinal relaxation time; **SD**, standard deviation; **FWHM**, full width at half maximum; **FID**, free induction decay; **Hz**, hertz; **SNR**, signal to noise ratio; **AMARES**, advanced method for accurate, robust and efficient spectral fitting; **PAD**, peripheral arterial disease; O_2, oxygen; **a.u.**, arbitrary units; **ISIS**, image-selected in vivo spectroscopy; **PRESS**, point resolved spectroscopy; **CSI**, chemical shift imaging; ^{1}H, proton; ^{31}P-MRS, phosphorus magnetic resonance spectroscopy; **μs**, microseconds.

the coefficient of variation (CV) and intra-class correlation coefficients (ICC), respectively. After sequence parameter optimization, Pi_{alk} demonstrated high intra-subject repeatability (CV: 10.6 ± 5.4%, ICC: 0.80). Proximo-distal change in coil position along the length of the quadriceps introduced Pi_{alk} quantitation variability (CV: 28 ± 5%), due to magnetic field inhomogeneity with more distal coil locations. In contrast, Pi_{alk} measurement variability due to repeated shims from the same muscle volume (0.40 ± 0.09mM; CV: 6.6%), and automated spectral processing (0.37 ± 0.01mM; CV: 2.3%), was minor. The quantification of Pi_{alk} in skeletal muscle via surface coil 31P-MRS at 3 T demonstrated excellent reproducibility. However, caution is advised against placing the coil at the distal part of the quadriceps to mitigate shimming inhomogeneity.

KEYWORDS
31P-MRS, mitochondria, mitochondrial biomarker, muscle energetics, muscle MR spectroscopy, repeatability

1 | INTRODUCTION

Since its early development in the 1970s, phosphorus magnetic resonance spectroscopy (^{31}P-MRS) has been integral to the study of skeletal muscle bioenergetics. A typical ^{31}P-MRS spectrum displays six prominent peaks corresponding to the three phosphate groups of adenosine triphosphate (ATP; β-ATP, α-ATP, and γ-ATP), phosphocreatine (PCr), the phosphodiesters (PDE) glycerophosphoethanolamine (GPE) and glycerophosphocholine (GPC), and inorganic phosphate (Pi). The advent of ultra-high field (>7 Tesla) whole-body scanners has reignited interest in the field of muscle bioenergetics, particularly in exploring skeletal muscle metabolites with low in vivo concentration (<1mM). Notably, compounds such as nicotinamide dinucleotide (NAD+) and an alkaline Pi resonance (Pi_{alk}) have garnered attention for their potential utility as markers of redox balance and mitochondrial content, respectively.

Early work in the field of ^{31}P-MRS identified a well-resolved Pi resonance in isolated mitochondria[1,2], which was later detected in perfused liver[3–5] and isolated heart[6,7] (i.e., organs rich in mitochondria). Specifically, a discernible doublet Pi peak was observed, with the upfield peak attributed to the cytosolic compartment (Pi_{cyt}), and the downfield more alkaline peak (Pi_{alk}) attributed to the mitochondrial matrix[1,3,4,6–8]. Carefully controlled experimental conditions ex vivo demonstrated that the signal amplitude of Pi_{alk} increased in response to mitochondrial swelling, and that its chemical shift varied according to the pH of the mitochondrial matrix[1–5]. Together, these studies conducted at ultra-high magnetic field ex vivo established the mitochondrial origin of an alkaline (~7.4–7.5) Pi pool[9,10].

In 2010, Kan et al, (2010) detected Pi_{alk} in vivo in resting human soleus and tibialis anterior (TA) muscles using a 7 T scanner[11]. This finding was then confirmed in the quadriceps muscles[12–14]. Importantly, several results in vivo corroborated the possible mitochondrial origin of Pi_{alk}. For instance, expressed as Pi_{alk}/Pi_{cyt}, a significantly lower ratio was documented in the TA (Pi_{alk}/Pi_{cyt}: 0.07; ~70% slow oxidative fibers) as compared to the soleus (Pi_{alk}/Pi_{cyt}: 0.11; ~90% slow oxidative fibers)[11], thus suggesting a greater mitochondrial content in the soleus, consistent with in vitro findings[15–17]. Similarly, aerobically trained athletes exhibited a higher Pi_{alk}/Pi_{cyt} ratio (0.07) in the quadriceps muscle than recreationally active adults (0.03)[13]. [Pi_{alk}] further correlated ($r = 0.68$) with the maximal rate of oxidative ATP synthesis (Q_{max}) as measured by ^{31}P-MRS in obese-to-sedentary patients, as well as lean active adults[12]. Together, these data suggest that Pi_{alk} is a candidate biomarker for quantifying mitochondrial content in the skeletal muscle.

However, ultra-high magnetic field scanners are rather scarce, which somewhat limits the translational impact of these findings. Although 3 T MR scanners are more broadly available, the short longitudinal relaxation time (T_1 < 1.5 s)[1,2,8,11], low concentration of Pi_{alk} in resting human skeletal muscle (<1mM), and close resonance proximity with the cytosolic Pi peak (~0.4 ppm) present a significant challenge to detect this metabolite at lower magnetic field. A necessary first step is to establish the methodology for a reproducible quantification of Pi_{alk} paving the way for its potential implementation in clinical trials in the future.

The primary objective of the current study was two-fold: (1) to assess the intra-subject absolute and relative repeatability of [Pi_{alk}] in the resting quadriceps of sedentary young adults, utilizing surface coil ^{31}P-MRS at 3 T, and (2) to evaluate the impact of changes in coil location, shimming optimization, and automated spectral processing on the measurement variability of [Pi_{alk}]. Using optimized parameters for its detection, we show that: (1) [Pi_{alk}] has a medium-to-strong absolute (i.e., low coefficient of variation) and relative (i.e., high intra-class coefficient of correlation) repeatability when measured at two separate time points separated by 7 days and (2) that shimming optimization and spectral processing minimally influence signal variability, but that coil placement is an important determinant in the variability of Pi_{alk} quantification.

2 | METHODS

2.1 | Participant characteristics

Following informed consent, 18 healthy young adults were enrolled for this study. Five (four males and one female) completed a set of experiments to optimize the sequence for P_{ialk} detection. After which, 13 (seven males and six females) completed the test–retest repeatability experiments. Participants were sedentary to moderately active, i.e. not engaged in structured physical activity more than three times a week, as confirmed by accelerometry. Habitual physical activity was characterized using uniaxial accelerometry (GT3X, Actigraph, Pensacola, FL) instrumented on the non-dominant wrist for seven days. All participants were non-smokers free from diabetes, and any known cardiovascular, peripheral vascular, neuromuscular, or pulmonary diseases, and not taking any medications known to alter metabolism. For the female participants, all tests were conducted within the first 7 days of the early follicular phase as sex hormones (i.e., estrogen and progesterone) are at their most stable during this period. The study was approved by the Institutional Review Board at the University of Massachusetts Amherst. All experimental trials were performed in a thermoneutral environment at the same time of day, with the subjects fasted overnight and having refrained from strenuous exercise for the past 24 hours. A comprehensive fasting blood panel was collected for complete blood cell count and lipid panel on the first experimental visit.

2.2 | T_1 characterization and sequence optimization

A critical step in assessing the repeatability of Pi_{alk} quantification at 3 T is to first optimize the sequence parameters to ensure that this metabolite can be detected at this field strength. For the following optimization scans, a custom-built $^{31}P/^{1}H$ surface circular coil (80 mm single loop ^{31}P coil surrounded by a 100 mm ^{1}H coil loop) with linear polarization was positioned mid-thigh above the right quadriceps muscle (Figure 1.) and scans performed within the bore of a 3 T whole-body MR scanner (Skyra, Siemens Healthineers, Erlangen, Germany). A set of ^{31}P progressive saturation experiments were then performed on three participants [repetition time (TR) = 550–2500 ms; 550, 1000, 1500, 2000, 2500 ms for a total of five points] using a pulse-acquire sequence with a 100 μs hard pulse and the following parameters: receiver bandwidth = 4 kHz, 2048 data points, nominal flip angle = 80°, 120 averages per spectrum, ^{1}H decoupling WALTZ-4 at 50%, i.e., 240 ms. Due to the short T_1 of Pi_{alk} and specific absorption rate (SAR) limit with the decoupling pulse, a second set of ^{31}P progressive saturation experiments was performed on two participants, at shorter TR (TR = 300, 500, 700, 900, 1100, 1300, 1500 ms) without ^{1}H decoupling to better characterize the longitudinal relaxation time (T_1) of Pi_{alk} at shorter TR. Additional experiments on these five participants were also conducted with varying pulse duration (100–300 μs), nominal flip angle (50–90°), and ^{1}H decoupling duration (96–288 ms).

2.3 | Intra-subject repeatability

Participants reported to the laboratory on two separate visits during a 7-day period (mean ± SD; 4 ± 2 days). To assess the *'test–retest repeatability'* of [Pi_{alk}], participants were instructed to lie supine within the bore of a 3 T whole-body MR scanner (Skyra, Siemens Healthineers, Erlangen, Germany) while resting concentration of phosphorylated compounds and intracellular pH were measured in the right quadriceps muscle.

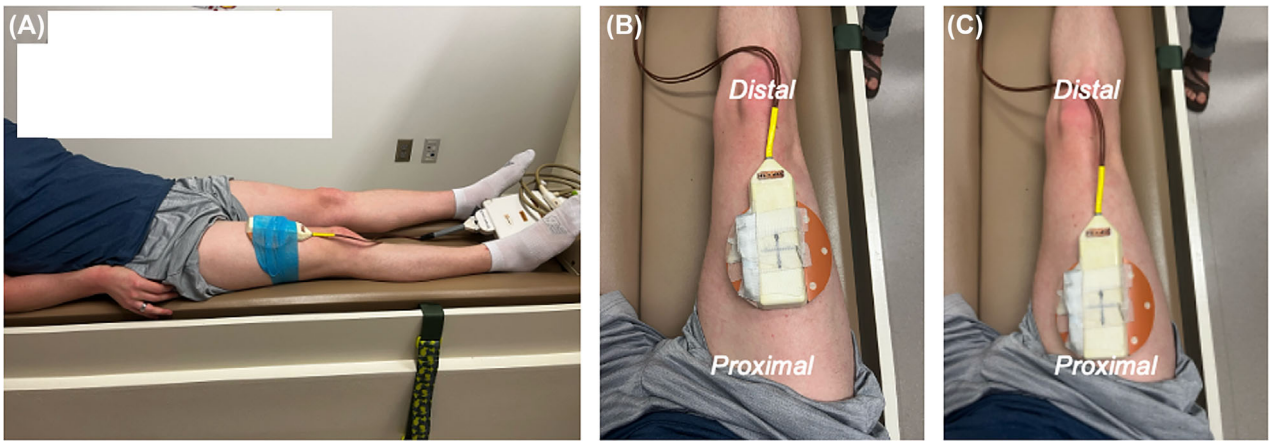

FIGURE 1 **Representative pictures of experimental setup and coil placement on thigh.** Participants were instructed to rest supine, with the quadriceps relaxed and coil positioned mid-thigh secured with coflex (**A.**). Representative image of coil placed at the mid-thigh (**B.**). Representative image of the coil placed proximally (closer to locations 5 and 6 when assessing *variability due to coil placement* (**C.**)

2.3.1 | ^{31}P-MRS acquisition

Three-plane scout proton MR images were initially acquired to determine the position of the leg with respect to the surface coil and to perform an automatic localized map shimming. Then, further optimization was performed via a manual shimming procedure [full width at half maximum (FWHM) for ^{1}H; Visit 1: 37.3 ± 5.4 and Visit 2: 37.2 ± 2.8 Hz; $p > 0.05$; for ^{31}P; Visit 1: 11.8 ± 0.8 and Visit 2: 11.6 ± 0.6 Hz; $p > 0.05$]. Unless stated otherwise, the ^{31}P MR spectrum was obtained with the following parameters: TR = 1500 ms, Bandwidth = 4000 Hz, 2048 data points, Nominal Flip Angle = 80°, 200 Averages, ^{1}H decoupling WALTZ-4 at 50% i.e., 240 ms, hard pulse 100 μs.

2.3.2 | ^{31}P-MRS analysis

Before signal fitting, the first time point of the free induction decay (FID) was corrected by adjusting the first order phase, and a 2 Hz Gaussian filter was applied to improve spectral resolution (e.g., to improve SNR without compromising spectral resolution). Relative concentrations of phosphocreatine [PCr], inorganic phosphate [Pi], phosphomonoester [PME], nicotinamide dinucleotide (NAD), and [ATP] were obtained by fitting their signals using Lorentzian line shapes with a time-domain fitting routine using the AMARES algorithm[18] incorporated into the CSIAPO software[19]. Prior knowledge for AMARES was constrained for Lorentzian line-shapes with Pi_{alk} frequency between 120 and 159 Hz, and damping of the FID decay to 0.003–0.09 KHz. Phase order was manually adjusted with a degree of tolerance of ± 3.6° for zero-phase order changes across the spectrum. Linewidth and peak area were left unconstrained. Cytosolic and alkaline pH were calculated from the chemical shift difference between PCr and the cytosolic and alkaline Pi signals, respectively. The resting concentrations were calculated assuming an 8.2 mM beta ATP concentration[20].

2.4 | Sources of measurement variability

2.4.1 | Coil position

In a subset of participants (n = 5), the coil was positioned on the quadriceps and moved along the length of the thigh in the distal-to-proximal direction to measure resting metabolites in six different locations. Coil placement was determined relative to the total thigh length, with a standardized gap of 16.7% of the total thigh length between each coil placement location, with automatic and manual shimming performed after each coil change (^{31}P full width at half maximum < 15 Hz).

2.4.2 | Shimming optimization

Measurement variability from an advanced localized automatic shimming followed by manual optimization of the shimming (^{31}P full width at half maximum <12 Hz) was calculated based on 10 consecutive scans acquired in the same location of the quadriceps on the same participant (n = 1; female; 23 yrs. old, 21.4 kg/m^2,8909 steps/day). The surface coil was positioned mid-thigh and the shimming procedure reset for each scan. The participant remained supine on the bed of the scanner throughout the entire procedure.

2.4.3 | Spectral processing and quantification

Analysis repeatability from post-processing of Pi_{alk} signal was estimated from one spectrum randomly selected in the dataset (n = 1) analyzed 20 times using a time-domain fitting routine[21] and the AMARES algorithm[18] incorporated into the CSIAPO software[19] and with the same prior knowledge for the metabolites of interest.

2.5 | Statistical analysis

Test–retest absolute and relative repeatability were analyzed using intra-subject coefficient of variation (CV) and intra-class correlation coefficients (ICC), respectively, as described previously[22]. Relative repeatability was defined as an individual maintaining his/her position, e.g., rank, within a sample with repeated measurements[23] and assessed with the ICC, a two-way random effects model with single measurement

repeatability in which variance over the repeated sessions is considered. The ICC indicates the error in measurements as a proportion of the total variance in scores. In accordance with Atkinson & Nevill, relative repeatability as assessed by the ICC was qualitatively defined as: ICC = 0.7–0.8 as 'questionable', ICC = 0.8–0.9 as 'good', and an ICC > 0.9 as 'high'[23].

Absolute repeatability is the degree to which repeated measurements vary for individuals and the measurement system[23]. This was performed by calculating the intra-subject (i.e., test–retest) and measurement procedure (i.e., coil positioning, repeated shims, automated spectral processing) CV, and then reporting the mean CV for the respective dependent variables. Accordingly, the intra-subject CV was calculated as the SD of the measurements recorded during both visits, or for each scan, and then divided by the mean of the two visits as previously described[22]. This assessment of CV is different from the inter-subject that quantifies the variability within the group rather than the intra-subject variability that requires a repeated measurement design. The corresponding result was expressed as a percentage. ICC and CV analyses was done using a downloadable Excel spreadsheet[22].

Statistical comparisons were performed, and figures generated, using open-source software (RStudio version 5.1.6, RStudio: Integrated Development for R, PBC, Boston, MA, USA). Boxplots were generated, with the bottom line representing the first quartile (>25% of the data), the middle dark line the median, and the top line the third quartile (>75% of the data). The dark square represents the mean and individual circles represent individual data points. Paired, two-tailed Wilcoxon-Signed Rank t-tests were conducted to assess a difference in mean [Pi_{alk}] between Visit 1 and 2. Pearson correlation was used for all correlation analysis. All data are presented as mean ± standard deviation (SD) unless stated otherwise.

3 | RESULTS

3.1 | Participant characteristics

Baseline participant characteristics for the repeatability protocol (males = 6; females = 7), including anthropometric, physical activity level, and blood profile are presented in Table 1.

3.2 | Sequence optimization and longitudinal relaxation time of Pi_{alk}

As illustrated in Figure 2A-C., the optimum pulse duration, nominal flip angle, and duration of the ^{1}H decoupling pulse were 100 μs, 80°, and 240 ms, respectively. The T_1 value of Pi_{alk} in the skeletal muscle in vivo was 412 ± 112 ms at 3 T (Figure 2D).

TABLE 1 Participant characteristics.

Sample size (female/male)	13 (7/6)	Range
Anthropometric characteristics		
Age (yrs)	22 ± 3	18–29
Height (cm)	172.9 ± 9.7	163–192
Mass (kg)	70.5 ± 12.8	51–91
BMI (kg/m^2)	23.6 ± 3.6	17.5–29.1
Physical activity		
Step Counts/Day	7812 ± 2432	3764–13,812
Blood and plasma characteristics		
Hemoglobin (g/dl)	14 ± 2	12–17
Hematocrit (%)	42 ± 5	37–50
Glucose (mg/dl)	87 ± 4	80–93
Total Cholesterol (mg/dl)	176 ± 34	116–225
HDL-C (mg/dl)	59 ± 15	42–86
LDL-C (mg/dl)	103 ± 23	55–125
Triglycerides (mg/dl)	72 ± 19	40–95

Abbreviations: BMI: Body Mass Index; HDL: High-Density Lipoprotein Cholesterol; LDL: Low-Density Lipoprotein Cholesterol.
Values are expressed as mean ± standard deviation (SD).

3.3 | Test–retest repeatability of Pi_{alk} and phosphate metabolites

An example of the MR spectra acquired from the quadriceps muscle is illustrated in Figure 3. Table 2 summarizes intracellular metabolite concentration and pH from both the cytosolic and alkaline Pi at rest. The resting concentrations of Pi_{alk} were 0.35 ± 0.09mM (visit 1) and 0.35 ± 0.10mM (visit 2), resulting in an intra-subject CV of 10.6 ± 5.4% and an ICC of 0.80 (Figure 4A., Table 2). The corresponding resting pH of Pi_{alk} was 7.46 ± 0.03 (visit 1) and 7.44 ± 0.03 (visit 2), resulting in an intra-subject CV of 0.2 ± 0.1% and an ICC of 0.74 (Table 2.). The resting Pi_{alk}/Pi_{cyt} ratio was 0.10 ± 0.03 for both visits, resulting in an intra-subject CV of 10.3 ± 8.1% and an ICC of 0.71 (Figure 4B., Table 2). Individual data of both visits for Pi_{alk} and Pi_{alk}/Pi_{cyt} are displayed in Figure 4D and4E, respectively. For comparison, Figure 4F and C represents the individual data of both visits for the well-resolved peak of PCr and ICC's, respectively.

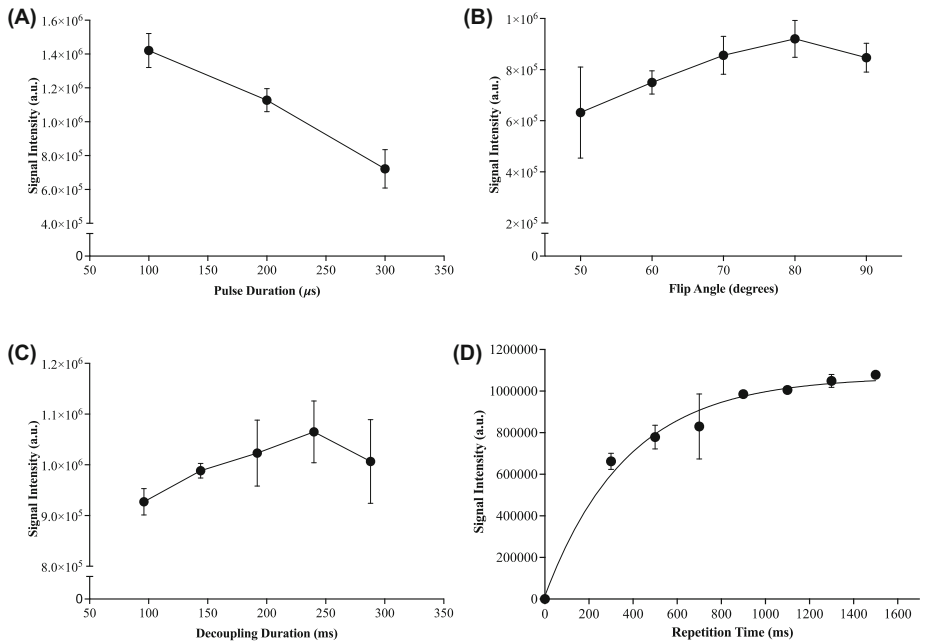

FIGURE 2 Sequence optimization for **(A.)** pulse duration, **(B.)** nominal flip angle, **(C.)**, ^{1}H decoupling pulse duration, and **(D.)** longitudinal relaxation time (T_1). Optimal values for pulse duration, nominal flip angle, and decoupling duration were 100 μs, 80°, and 240 ms, respectively. T_1 value of Pi_{alk} in the skeletal muscle in vivo was 412 ± 112 ms. n = 5.

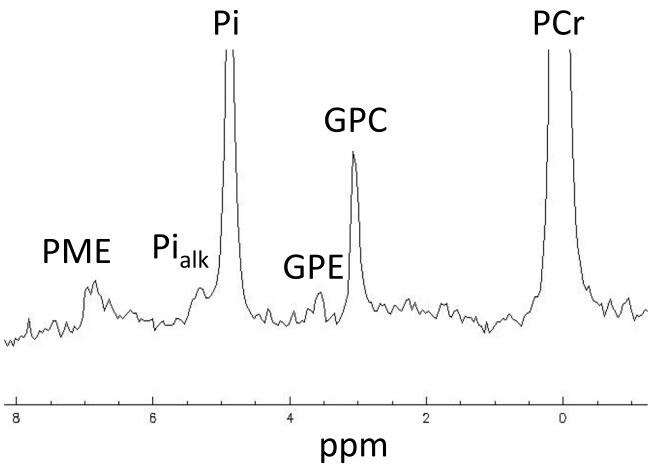

FIGURE 3 Representative example of a ^{31}P-MRS spectra in the quadriceps muscle of a healthy young adult at 3 T, with the region between 0 and 8 ppm enlarged. The signal-to-noise-ratio was 11, 39, and 507 for Pi_{alk}, pi cytosolic, and PCr, respectively. A 2 Hz Gaussian filter was used for apodization. **PCr**: phosphocreatine; **GPC**: Glycero-3-Phosphocholine; **GPE**: Glycero-3-Phosphoethanolamine; **pi**: cytosolic inorganic phosphate; **Pi_{alk}**: alkaline inorganic phosphate; **PME**: Phosphomonoesters.

TABLE 2 Intra-subject repeatability in ^{31}P-MRS variables at rest.

Resting metabolite	Visit 1	Range visit 1	Visit 2	Range visit 2	Mean CV (%)	ICC (95% CI)
PCr (mM)	37.2 ± 3.1	32.5–43.1	36.9 ± 3.1	31.3–42.3	3.3 ± 2.2	0.77 (0.77,0.768)
Pi_{cyt} (mM)	3.6 ± 0.7	2.9–5.6	3.5 ± 0.6	2.9–5.3	5.9 ± 4.4	0.84 (0.84,0.837)
Pi_{alk} (mM)	0.35 ± 0.09	0.35–0.50	0.35 ± 0.10	0.20–0.50	10.6 ± 5.4	0.80 (0.80,0.804)
PDE (mM)	1.80 ± 0.42	1.09–2.40	1.68 ± 0.42	1.04–2.40	5.7 ± 5.7	0.94 (0.94,0.936)
Total NAD (mM)[1]	1.11 ± 0.23	0.89–1.50	1.31 ± 0.32	0.87–1.30	14.4 ± 0.2	0.23 (0.23,0.231)
Pi_{alk}/Pi_{cyt}	0.10 ± 0.03	0.05–0.20	0.10 ± 0.03	0.06–0.20	10.3 ± 8.1	0.71 (0.71,0.708)
β-ATP (a.u.)	65,431 ± 14,522	42,800–84,000	60,322 ± 20,330	9960–83,300	11.4 ± 29.6	0.41 (0.41,0.409)
pH Cytosolic	6.97 ± 0.02	6.94–7.00	6.97 ± 0.02	6.94–7.00	0.1 ± 0.1	0.64 (0.64,0.640)
pH alkaline	7.46 ± 0.03	7.41–7.50	7.44 ± 0.03	7.39–7.50	0.2 ± 0.1	0.74 (0.74,0.745)

Abbreviations: PCr: Phosphocreatine; Pi: Inorganic Phosphate; Pi_{alk}: Alkaine Inorganic Phosphate; Pi_{cyt}: Cytosolic Inorganic Phosphate; PDE: Phosphodiesters; NAD: Nicotinamide Adenine Dinucleotide; β-ATP: Beta Peak of Adenosine Triphosphate; a.u.: Arbitrary Units; CV: coefficient of variation; ICC: Intraclass Coefficient of Variation; CI: 95% lower and upper confidence intervals.
Values are expressed as mean ± SD. Sample size = 13.
[1]Total NAD includes NAD + and NADH.

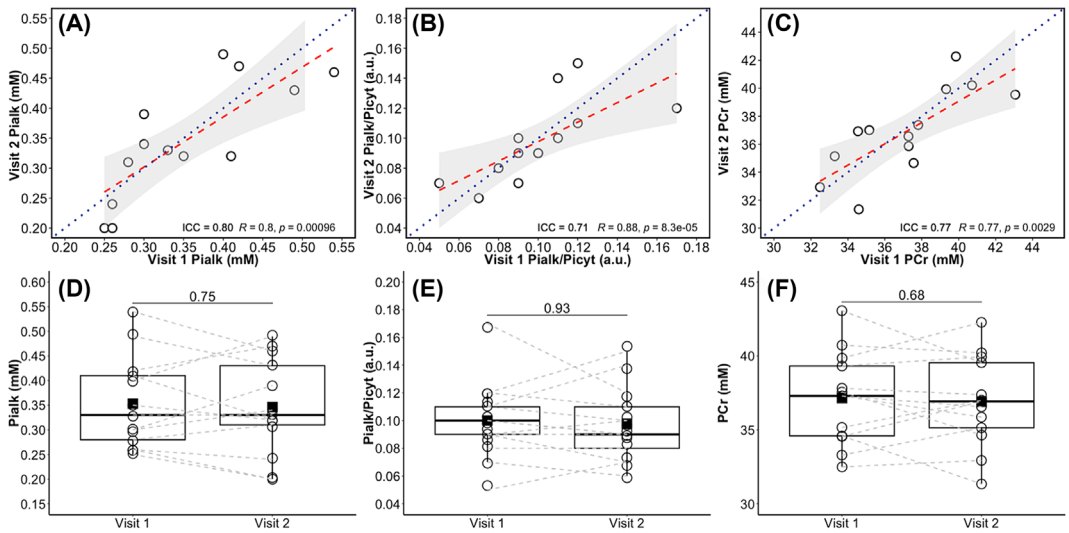

FIGURE 4 Top three panels are the corresponding scatter plots for Pi_{alk} **(A.)**, Pi_{alk}/Pi_{cyt} **(B.)**, and PCr **(C.)** comparing visit 1 and visit 2. Dotted blue lines represent the *'line of identity'*. Shaded light gray region is the 95% confidence interval. Dashed red lines is the regression line. Bottom three panels represent the means and individual data points for Pi_{alk} (visit 1: 0.35 ± 0.09mM vs. visit 2: 0.35 ± 0.10mM; **D.)**, Pi_{alk}/Pi_{cyt} (visit 1: 0.10 ± 0.03 a.u. vs. visit 2: 0.01 ± 0.03 a.u.; **E.)**, and PCr (visit 2: 37.15 ± 3.09 vs. 31.34 ± 3.06mM; **F.)**. N = 13. **ICC:** intraclass correlation coefficient **mM:** millimolar concentration; **a.u.:** arbitrary units.

3.4 | Effect of coil location on Pi_{alk} measurement variability

When the coil was positioned on the quadriceps and moved along the length of the thigh in the distal-to-proximal direction, the CV across all six positions for Pi_{alk} was 28 ± 5% (Table 3). In contrast, the CV across all six positions for Pi, PCr, PDE, the pH of $Pi_{alkaline}$, and the pH of $Pi_{cytoplam}$ were lower with values of 8 ± 4%, 7 ± 4%, 8 ± 3%, 0.49 ± 0.11%, and 0.13 ± 0.09, respectively (Table S1). It is noteworthy that the shimming quality deteriorated in the region closer to the knee as indicated by the higher FWHM (>13 Hz, Figure 4).

3.5 | Effect of shimming on Pi_{alk} measurement repeatability

The CV for Pi_{alk} in 10 consecutive scans, during which the shimming procedure was reset each time, was 6.6% (Table 3). For comparison, Table 3 summarizes the intracellular concentration of other well-resolved phosphorus metabolites and pH, along with their respective CVs, following the same procedure.

TABLE 3 Repeatability related to coil position, intra-session repeated shims, and spectral processing.

	PCr (mM)	Pi (mM)	Pi_{alk} (mM)	PDE (mM)	$pH_{Cytoplasm}$	$pH_{alkaline}$
a. Effect of coil position (n = 5)						
Metabolic variable (% CV)	34.5 ± 2.5 (7 ± 4)	3.7 ± 0.2 (8 ± 4)	0.40 ± 0.09 (28 ± 5)	1.98 ± 0.04 (8 ± 3)	6.98 ± 0.01 (0.13 ± 0.09)	7.45 ± 0.02 (0.49 ± 0.11)
b. Intra-session repeatability (n = 1, 10 repeated measurements with new shimming)						
Metabolic variable (% CV)	29.1 ± 0.4 (1.5)	3.0 ± 0.1 (3.0)	0.40 ± 0.03 (6.6)	2.19 ± 0.04 (1.7)	6.99 ± 0.00 (0.1)	7.44 ± 0.02 (0.3)
c. Repeatability of spectral processing (n = 1, 20 repeated measurements)						
Metabolic variable (% CV)	32.2 ± 0.2 (0.7)	2.7 ± 0.0 (0.7)	0.37 ± 0.01 (2.3)	1.19 ± 0.01 (0.9)	6.98 ± 0.00 (0.0)	7.43 ± 0.00 (0.0)

Values are expressed as mean ± SD, with the coefficients of variation (CV) in parentheses.

3.6 | Effect of spectral processing on Pi_{alk} and ^{31}P metabolites repeatability

The analysis repeatability CV was 6.6% for Pi_{alk} in one spectrum that was randomly selected, with spectral post-processing repeated 20 times. For comparison, Table 3 summarizes the intracellular concentration of other well-resolved phosphorus metabolites and pH, along with their respective CVs, following the same procedure.

4 | DISCUSSION

The aim of the present study was twofold: (1) to quantify the intra-subject test–retest absolute and relative repeatability of Pi_{alk} measured by ^{31}P-MRS in resting quadriceps muscle of healthy young adults using a surface coil at 3 T, and (2) to determine the potential factors contributing to [Pi_{alk}] variability (i.e., coil placement, shimming, and automated spectral processing error). Using a sequence with a short TR coupled to ^{1}H decoupling, resting [Pi_{alk}] was ~0.35mM in the quadriceps of healthy young adults, and demonstrated good repeatability with a test–retest CV of 10.6%. Importantly, shimming (CV = 6.6%) and spectral processing (CV ≤ 2.3%) accounted for a limited portion of Pi_{alk} measurement variability. In contrast, coil location affected Pi_{alk} quantification (CV: 28 ± 5%), with higher [Pi_{alk}] in the distal region of the thigh (i.e., closest to the patella), likely due to magnetic field inhomogeneity in the sampled area. Collectively, the present study supports the repeatability of Pi_{alk} quantification in the skeletal muscle by ^{31}P MRS using ^{1}H decoupling and a surface coil at 3 T, as long as magnetic field homogeneity is optimized (FWHM of PCr < 12.5 Hz).

4.1 | Technical considerations for the measurement of Pi_{alk}

Several aspects needed to first be considered to optimize the spectral resolution of Pi_{alk} and thus ensure sufficient reproducibility. The T_1 of the alkaline Pi resonance measured in isolated mitochondria (T_1 = 540 ms[24]; T_1 = 600 ms[1]) and perfused liver in situ (T_1 = 710 ms[8]) at ultra-high magnetic field (9.4 T) was very short. This value was 1.4 ± 0.5 s in the skeletal muscle in vivo at 7 T[11] and the T_1 of Pi_{alk} in the present study was 412 ± 112 ms (Figure 2D) using a progressive saturation technique. Together, both in vivo studies concur that the T1 relaxation of Pi_{alk} is shorter than the T1 of cytosolic Pi, thus extending prior findings in isolated tissues. Of note, previous studies in humans used longer TRs (4–5 s[11,14] and 15 s[12,25,26]), resulting in lower saturation of the cytosolic Pi, and thus greater overlap in the signal of the two Pi pools. The faster pulsing conditions (TR = 1.5 s) used in the present study thus provided several advantages by allowing a better splitting between the cytosolic with a longer T_1 (~7 s)[27] and alkaline Pi peaks, more signal averaging to improve the signal-to-noise ratio (SNR) while keeping a reasonable acquisition time (acquisition time ~5 min in the present study). The prolonged irradiation (250 ms) of the ^{1}H coupled to ^{31}P using a decoupling pulse Waltz-4 improved the signal intensity of Pi_{alk} by ~17% (data not shown) along with its spectral resolution without reaching SAR limits. Such enhancement in the signal has previously been demonstrated to improve the repeatability of metabolite measurements[28], which was even more critical given the low concentration of Pi_{alk}. Finally, the use of a small surface coil provided greater signal sensitivity for superficial tissue such as the quadriceps compared to a volume coil (e.g., birdcage). This coil design may, however, be problematic for other muscle groups with heterogeneous fiber type composition (e.g., plantar flexor muscles). Together, these optimization steps contributed to a more accurate detection of Pi_{alk} despite its low concentration in the skeletal muscle and small chemical shift difference with the cytosolic Pi (~0.4 ppm).

4.2 | Pi_{alk} concentration in the quadriceps muscle at rest

Utilizing this optimized setup, the concentration of Pi_{alk} in the quadriceps of healthy sedentary to moderately active young adults was approximately 0.35mM (Table 2, Figure 4). This concentration falls within the range of values previously measured in the quadriceps and plantar flexor muscles of untrained healthy young adults at 7 T (~0.28–0.42mM)[1,12,17]. Interestingly, quadriceps [Pi_{alk}] in the present study was slightly lower than [Pi_{alk}] of the vastus lateralis of endurance-trained athletes[17], but two-fold higher than values reported in obese individuals (~0.18mM)[12], which may be consistent with the mitochondrial origin of this Pi pool. In contrast, Sedivy and colleagues reported higher [Pi_{alk}] in the plantar flexor muscles of healthy older individuals (~0.8mM) and values as high as ~3.0mM in patients with peripheral arterial disease (PAD) at 3 T[24]. The reason for this discrepancy is unclear, but it should be noted that both studies employed different acquisition parameters (TR = 1.5 s in the present study vs. 15 s, signal averaging = 200 in the present study vs. 16), which may have led to signal overlap and potential overestimation of [Pi_{alk}] in the study by Sedivy and colleagues. Also, patients with PAD and intermittent claudication may exhibit higher mitochondrial content than their healthy counterparts to compensate for poor mitochondrial function or low O_2 availability [29,30], which may translate into higher [Pi_{alk}] if the Pi pool originates from the mitochondrial matrix[11,13]. Alternatively, Sedivy et al suggested that tissue edema, commonly observed in the lower limb of PAD patients could have contribute to an increased [Pi_{alk}] in this population if the Pi pool is located in the interstitium. Therefore, both technical and fundamental physiological factors may explain the differences in [Pi_{alk}] between studies.

4.3 | Intra-subject test–retest repeatability of Pi_{alk}

A central finding of the present study was the observation of both high absolute repeatability (CV = 10.6 ± 5.4%) and good relative repeatability (defined as an ICC ranging from 0.80–0.90) for [Pi_{alk}]. As expected, Pi_{alk} repeatability assessed by the CV was slightly lower than well-resolved metabolites e.g., PCr, Pi, PDE (CV: ~3–6%). However, these same well-resolved metabolites had ICC values similar to Pi_{alk} (ranging from 'good' to 'high' relative reproducibility; see Table 2.). It is noteworthy that despite the large differences in concentration between Pi_{alk} and the other metabolites (e.g., PCr was ~80 fold higher, Pi ~7 fold higher, and PDE ~ 4 fold higher than Pi_{alk}) the metrics of absolute and relative repeatability were high. Importantly, they were within a close range to these well-resolved metabolites supporting that Pi_{alk} can be robustly and reproducibly quantified at 3 T. To put this in perspective, studies conducted at a similar field strength (i.e., 3 T) reported CVs for cytosolic Pi of 15% in the tibialis anterior muscle with a 10-day intra-subject test–retest design[31] and 8% in the plantar flexor muscles with a 7-day intra-subject test–retest design[17]. Only two studies calculated the ICC of ^{31}P metabolites and reported values of 0.79[17] and 0.14[22] for cytosolic Pi in the plantar flexor muscles (measured one week apart) and quadriceps (measured two months apart), respectively. Collectively, these findings suggest that Pi_{alk} can be reliably quantified in the quadriceps at 3 T, with repeatability similar to other well-studied phosphate metabolites (e.g., PCr, Pi, PDE).

4.4 | Measurement variability: effect of coil location and field homogeneity on Pi_{alk} quantification

The effects of coil placement and intra-session repeated shims were evaluated to further determine the potential factors contributing to the variability in Pi_{alk} quantification. When the coil position was shifted along the thigh in the distal-to-proximal direction, a CV of 28 ± 5% was observed for Pi_{alk} (Table 3). This is somewhat in contrast to the other well-resolved metabolites, e.g., PCr (CV = 7 ± 4%) and Pi (CV = 8 ± 4%), which were less affected by coil placement. Given the close spectral proximity of Pi_{alk} to the cytosolic Pi, Pi_{alk} was poorly resolved and difficult to quantify in all participants for position 1 (17% of femur length from the knee), and in 5/6 participants for position 2 (33% of femur length from the knee). When positions 1 and 2, which displayed a higher FWHM than other coil locations, were excluded from the analysis, the CV for Pi_{alk} decreased to 16 ± 14% (Supplemental Table 1.), a near 50% decrease in variability.

The low repeatability along the length of the thigh is likely due to a change in coil loading/shimming quality. The FWHM of PCr, which was used to evaluate the homogeneity of the magnetic field in the sampled area, was higher at 16.6% and 33.3% of the total thigh length (~13–14 Hz, Figure 5). This larger linewidth may have resulted in an overlap with the cytosolic Pi signal and thus led to Pi_{alk} signal overestimation during spectral fitting. In contrast, other well-resolved and higher-signal magnitude metabolites (PCr, Pi, ATP) were less susceptible to this small decrease in shimming quality, as indicated by their unchanged concentration. Given the influence of magnetic field inhomogeneity on spectral resolution for Pi_{alk} quantification, we also evaluated measurement variability related to shimming within a session. Localized map shimming using an advanced automatic shimming algorithm combined with manual shimming to fine-tune the gradients (FWHM <12.5 Hz) was repeated prior to scanning the same participant and resulted in 'excellent' absolute repeatability for Pi_{alk} (CV = 2.3%, Table 3) when the coil was placed mid-thigh. This value was of a similar magnitude as for PCr (CV = 1.5%), Pi (CV = 3.0%), PDE (CV = 1.7%), and pH (CV = 0.1–0.3%).

Interestingly, the sum of the phosphate signals (Pi, PDE, PCr, ATP) was ~27% lower at coil placement 1 (~240,000 a.u.) than the other coil placements (~332,000 a.u., Supplemental Table 1.), indicating potential differences in the composition of the tissue underneath the coil (e.g., greater connective tissue content and lower muscle volume in the coil). Conceptually, the observed disparity in [Pi_{alk}] along the length of the

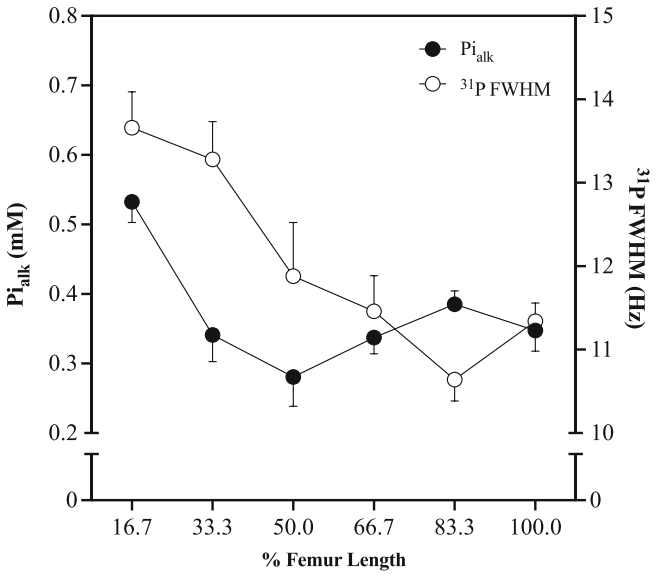

FIGURE 5 [Pi_{alk}] across six different coil placements (right y-axis) plotted in relation to the forward width half maximum of ^{31}P (FWHM; left y-axis). The six different *'sample volumes'* were measured along the longitudinal length of the quadriceps, with a distance of 16.7% of total thigh length between coil placements, starting at the patella and with the muscle fully relaxed. FWHM = full width half maximum of PCr. Sample size = 5.

thigh may thus also arise from differences in muscle fiber properties in the sampled region[28,32]. Oxidative type I muscle fibers (as compared to glycolytic type II fibers) would be expected to have a higher [Pi_{alk}] provided this is a surrogate marker of mitochondrial content. Although the present study was not designed to investigate an effect of muscle composition on [Pi_{alk}] repeatability, a recent study by Horwath et al reported no differences in fiber type along the longitudinal length of the vastus lateralis using muscle biopsies, ruling out any potential effect of muscle fiber typology[33].

Together, these results emphasize the critical role of coil placement and optimization of magnetic field homogeneity for achieving better spectral resolution and consistent Pi_{alk} quantification using a surface coil. Notably, it is recommended that surface coil placement be confined to the top 2/3 of the thigh muscle (i.e., starting at 33.3% of total femur length measured from distal-to-proximal) to ensure sufficient magnetic field homogeneity. Alternatively, strategies relying on single-voxel (e.g., ISIS, PRESS) or multi-voxel (2D-CSI) pulse sequence localization may be used, however, at the expense of maintaining high SNR.

4.5 | Effect of spectral processing on Pi_{alk} quantification

Using a time-domain fitting routine and the AMARES algorithm[18], with the same prior knowledge of the metabolites of interest incorporated into the CSIAPO software[19] (Pi_{alk} peak frequency range 125–160 Hz), the quantification of all major phosphate metabolites was highly reproducible (i.e., 'excellent') with CVs generally below 1%, and a maximum of 2.3% for Pi_{alk}. These values are similar to a previous study by our group at 1.5T[22] that used the same post-processing procedure, thus confirming the robustness of this approach for quantifying metabolites compared to manual curve fitting[26].

4.6 | Perspective: is Pi_{alk} a biomarker of mitochondrial content?

Collectively, the high absolute and relative repeatability of [Pi_{alk}] suggests that this measurement is suitable to monitor longitudinal changes and for cross-sectional comparisons in skeletal muscle groups with a mixed fiber type, such as the quadriceps. Interestingly, besides being located to the mitochondrial matrix[1,3,4,6–8], recent ^{31}P MRS magnetization transfer experiments demonstrated that this alkaline Pi pool exhibited low metabolic activity and did not participate in ATP synthesis[14]. It was also correlated to skeletal muscle oxidative phosphorylation capacity[12,13], which suggests that this metabolite may be used as a biomarker of mitochondrial content. These findings present, however, some limitations as both studies used a cross-sectional design (athletes or obese individuals versus age-matched controls) and were limited in sample size. In the present study, both the short T_1 and pH (7.39–7.5) of the alkaline Pi pool were consistent with a mitochondrial origin for this signal[1,3,4,6–8]. However, in

the absence of a direct comparison of mitochondrial content with [Pi_{alk}], it cannot be ruled out that this Pi pool might originate from the interstitium[14,24]. As mitochondria-targeted therapies have garnered a growing interest from the clinical community, the need for reliable biomarkers of mitochondrial properties to evaluate treatment effectiveness has become more pressing. The current study represents a crucial first step toward validating [Pi_{alk}] as a biomarker of mitochondrial content. It achieves this by demonstrating its repeatability and providing guidelines for future studies to accurately detect this metabolite in skeletal muscle at 3 T.

5 | CONCLUSION

The present study provides robust evidence that Pi_{alk} demonstrates an excellent absolute and relative reproducibility, similar to larger phosphate metabolites (e.g., PCr). This finding is a pre-requisite for Pi_{alk} to be sensitive to both longitudinal changes (i.e., intra-subjects) and cross-sectional analysis (i.e., between-subject changes). An important aspect to consider is the placement of the surface coil on the thigh to ensure sufficient shimming quality. Specifically, coil placement closer to the knee, were associated with higher magnetic field inhomogeneity, and demonstrated higher [Pi_{alk}] caused by poor signal quality and inaccurate quantification from the greater overlap between Pi_{alk} and cytosolic Pi. Provided that sufficient shimming quality is achieved, the quantification of Pi_{alk} using a fitting algorithm such as AMARES yields to highly reproducible results. Collectively, the present investigation supports the potential application of Pi_{alk} in research and clinical settings. Future studies are needed to directly evaluate the relationship between Pi_{alk} and mitochondrial content in both healthy and clinical populations (e.g., older adults), which is the next step that needs to be accomplished for the future implementation of this measure in clinical trials.

DATA AVAILABILITY STATEMENT

The data that support the findings of this study are available from the corresponding author upon reasonable request.

REFERENCES

1. Ogawa S, Rottenberg H, Brown T, Shulman R, Castillo C, Glynn P. High-resolution 31P nuclear magnetic resonance study of rat liver mitochondria. *Proc Natl Sci USA*. 1978;75:1796-1800.
2. Hutson S, Williamson G, Berkich D, LaNoue K, Briggs R. A 32P NMR study of mitochondrial inorganic phosphate visibility: effects of Ca2+, Mn2+, and the pH gradient. *Biochemistry*. 1992;31(5):1322-1330.
3. Cohen S, Ogawa S, Rottenberg H, et al. 31P nuclear magnetic resonance studies of isolated rat liver cells. *Nature*. 1978;273(5663):554-556.
4. Thiaudiere E, Gallis J, Dufour S, Rousse N, Canioni P. Compartmentation of inorganic phosphate in perfused rat liver can cytosol be distinguished from mitochondria by 31PNMR? *FEBS Lett*. 1993;330(2):231-235.
5. Vidal G, Gallis J, Canioni P. NMR studies of inorganic phosphate compartmentation in the isolated rat liver during acidic perfusion. *Arch Biochem Biophys*. 1997;337(2):317-325.
6. Garlick P, Brown T, Sullivan R, Ugurbil K. Observation of a second phosphate Pool in the perfused heart by 31P NMR; is this the mitochondrial phosphate? *J Mol Cell Cardiol*. 1983;15(12):855-858.
7. Garlick P, Soboll S, Bullock G. Evidence that mitochondrial phosphate is visible in 31PNMR spectra of isolated, perfused rat hearts. *NMR Biomed*. 1992;5(1):29-36.
8. Dufour S, Thiaudiere E, Vidal G, Gallis J, Rousse N, Canioni P. Temperature dependence of NMR relaxation times of nucleoside triphosphates and inorganic phosphate in the isolated perfused rat liver. Effect on pi compartmentation. *J Magn Reson B*. 1996;113(2):125-135.
9. Toth A, Meyrat A, Stoldt S, et al. Kinetic coupling of the respiratory chain with ATP synthase, but not proton gradients, drives ATP production in cristae membranes. *Proc Natl Acad Sci U S a*. 2020;117(5):2412-2421. doi:10.1073/pnas.1917968117
10. Orij R, Postmus J, Ter Beek A, Brul S, Smits GJ. Measurement of cytosolic and mitochondrial pH using a pH-sensitive GFP derivative in reveals a relation between intracellular pH and growth. *Microbiol-Sgm*. 2009;155:268-278.
11. Kan HE, Klomp DW, Wong CS, et al. In vivo 31P MRS detection of an alkaline inorganic phosphate pool with short T1 in human resting skeletal muscle. *NMR Biomed*. 2010;23(8):995-1000. doi:10.1002/nbm.1517
12. Valkovic L, Chmelik M, Ukropcova B, et al. Skeletal muscle alkaline Pi pool is decreased in overweight-to-obese sedentary subjects and relates to mitochondrial capacity and phosphodiester content. *Sci Rep*. 2016;6:20087.
13. van Oorschot JW, Schmitz JP, Webb A, Nicolay K, Jeneson JA, Kan HE. 31P MR spectroscopy and computational modeling identify a direct relation between pi content of an alkaline compartment in resting muscle and phosphocreatine resynthesis kinetics in active muscle in humans. *PLoS ONE*. 2013;8:e76628.
14. Wary C, Naulet T, Thibaud J, Monnet A, Blot S, Carlier P. Splitting of Pi and other 31P NMR anomalies of skeletal muscle metabolites in canine muscular dystrophy. *NMR Biomed*. 2012;25(10):1160-1169. doi:10.1002/nbm.2785
15. Forbes SC, Slade JM, Francis RM, Meyer RA. Comparison of oxidative capacity among leg muscles in humans using gated 31P 2-D chemical shift imaging. *NMR Biomed*. 2009;22(10):1063-1071. doi:10.1002/nbm.1413
16. Gregory C, Vandenborne K, Dudley G. Metabolic enzymes and phenotypic expression among human locomotor muscles. *NMR Biomed*. 2001;24:387-393.
17. Klepochova R, Valkovic L, Hochwartner T, et al. Differences in muscle metabolism between triathletes and normally active volunteers investigated using multinuclear magnetic resonance spectroscopy at 7T. *Front Physiol*. 2018;9:300.
18. Vanhamme L, van den Boogart A, Van Huffel S. Improved method for accurate and efficient quantification of MRS data with use of prior knowledge. *J Magn Reson*. 1997;129(1):35-43.

19. Le Fur Y, Nicoli F, Guye M, Confort-Gouny S, Cozzone PJ, Kober F. Grid-free interactive and automated data processing for MR chemical shift imaging data. *Magma*. 2010;23(1):23-30. doi:10.1007/s10334-009-0186-y
20. Meyerspeer M, Boesch C, Cameron D, et al. 31P magnetic resonance spectroscopy in skeletal muscle: Experts' consensus recommendations. *NMR Biomed*. 2020;34(5):e4246. doi:10.1002/nbm.4246
21. van der Veen A, Vanderveen M, Paulraj A. *Joint angle and delay estimation using shift-invariance techniques*. Vol. 46. IEEE; 1998:405-418.
22. Layec G, Bringard A, Le Fur Y, et al. Repeatability assessment of metabolic variables characterizing muscle energetics in vivo: a 31P-MRS study. *Magn Reson Med*. 2009;62(4):840-854. doi:10.1002/mrm.22085
23. Atkinson G, Nevill AM. Statistical methods for assessing measurement error (reliability) in variables relevant to sports medicine. *Sports Med*. 1998; 26(4):217-238.
24. Sedivy P, Dezortova M, Drobny M, et al. Origin of the (31) P MR signal at 5.3 ppm in patients with critical limb ischemia. *NMR Biomed*. 2020;33: e4295.
25. Lagemaat MW, van de Bank BL, Sati P, Li S, Maas MC, Scheenen TW. Repeatability of (31) P MRSI in the human brain at 7 T with and without the nuclear Overhauser effect. *NMR Biomed*. 2016;29(3):256-263. doi:10.1002/nbm.3455
26. Miller R, Carson P, Moussavi R, et al. Factors which influence alterations of phosphates and pH in exercising human skeletal muscle: measurement error, reproducibility, and effects of fasting, carbohydrate loading, and metabolic acidosis. *Muscle Nerve*. 1995;18(1):60-67.
27. Bogner W, Chmelik M, Schmid A, Moser E, Trattnig S, Gruber S. Assessment of 31P relaxation times in the human calf muscle: a comparison between 3 T and 7 T in vivo 2009. *Magn Reson Med*. 2009;62(3):574-582. doi:10.1002/mrm.22057
28. Boss A, Heskamp L, Breukels V, Bains LJ, van Uden MJ, Heerschap A. Oxidative capacity varies along the length of healthy human tibialis anterior. *J Physiol*. 2018;596(8):1467-1483. doi:10.1113/JP275009
29. Angquist K, Sjostrom M. Intermittent claudication and muscle fiber fine structure: morphometric data on mitochondrial volumes. *Ultrastruct Pathol*. 1980;1(4):461-470.
30. Elander A, Sjostrom M, Lundgren F, Schersten T, Bylund-Fellenius A. Biochemical and morphometric properties of mitochondrial populations in human muscle fibres. *Clin Sci (Lond)*. 1985;69:153-164.
31. Kolkovsky A, Marty B, Giacomini E, Meyerspeer M, Carlier P. Repeatability of multinuclear interleaved acquisitions with nuclear Overhauser enhancement effect in dynamic experiments in the calf muscle at 3T. *Magn Reson Med*. 2021;86:115-130.
32. Heskamp L, Lebbink F, van Uden MJ, et al. Post-exercise intramuscular O(2) supply is tightly coupled with a higher proximal-to-distal ATP synthesis rate in human tibialis anterior. *J Physiol*. 2021;599(5):1533-1550. doi:10.1113/JP280771
33. Horwath O, Envall H, Roja J, et al. Variability in vastus lateralis fiber type distribution, fiber size, and myonuclear content along and between the legs. *J Appl Physiol*. 2021;131(1):158-173. doi:10.1152/japplphysiol.00053.2021

SUPPORTING INFORMATION

Additional supporting information can be found online in the Supporting Information section at the end of this article.

How to cite this article: Matias AA, Serviente CF, Decker ST, et al. Repeatability of alkaline inorganic phosphate quantification in the skeletal muscle using ^{31}P-magnetic resonance spectroscopy at 3 T. *NMR in Biomedicine*. 2024;37(12):e5255. doi:10.1002/nbm.5255